

CHAPTER 149

PREDICTION OF TURBIDITY CURRENTS WITH BOUSSINESQ VISCOSITY AND SECOND-MOMENT CLOSURE MODELS.

Bård Brørs¹ and Karl J. Eidsvik¹

ABSTRACT

Sediment auto-suspension criteria (specifying the limit between eroding, self-accelerating flow and depositing, decelerating flow depending on the slope angle and particle settling velocity) differ by two orders of magnitude for different models in use. Experiments suggest that the results from ordinary density currents are applicable to turbidity currents. In the present study, models based upon well-known turbulence closures are applied in order to obtain a realistic description of turbidity currents:

A two-equation ($k-\varepsilon$) model predicts phase plane behaviour in accordance with results from theoretical work reported in the literature, and with limits for auto-suspension within the range of conventional estimates. However, by its design, this model and simpler gradient diffusion models are unable to produce turbulent diffusion of sediments up through the level of the velocity maximum.

A model with second-moment Reynolds stress turbulence closure is applied. This model proves to overcome the problem of vanishing turbulent diffusivity in the velocity maximum and give plausible results for vertical distribution of flow parameters in turbidity currents.

INTRODUCTION

Turbidity currents belong to the class of flows called gravity currents. A turbidity current is forced by the down-slope component of the gravitational acceleration acting on the soaring sediment grains, which in turn are kept in suspension by the turbulence generated by the current itself. Turbidity currents on the sea-bottom are known to have travelled hundreds of kilometers at speeds of more than 25 m/s and to have left turbidites (sediment deposits) of over 100 km³. The present study considers the portion of the flow well behind the advancing front, where horizontal gradients of flow variables may be ignored. Figure 1 shows a sketch

¹Norwegian Hydrotechnical Laboratory, N-7034 Trondheim, Norway.

of the situation with suggested mean velocity and mean concentration profiles. As long as the slope is sufficiently steep and sediments are available, the flow increases its height, velocity and amount of sediments in suspension. For this

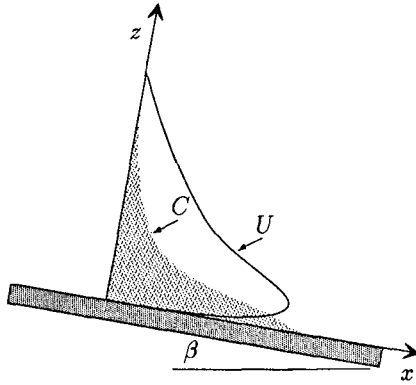


Figure 1: Turbidity current sketch.

shallow near-to-uniform flow, the thin shear layer approximation can be made, the equations for the mean velocity U and mean sediment concentration C may be written

$$\frac{\partial \rho U}{\partial t} = \frac{\partial \tau}{\partial z} + (\rho_s - \rho_f) C g \sin \beta, \tag{1}$$

$$\frac{\partial C}{\partial t} = -\frac{\partial}{\partial z} (\overline{cw} - w_T \cos \beta C). \tag{2}$$

Here, ρ_s and ρ_f are the solid and fluid densities and w_T is the particle settling velocity (positive downwards) and g is the gravitational acceleration.

Sediment auto-suspension criteria differ by two orders of magnitude for different models in use (Seymour, 1986). It is a limited supply of data for model verification, but experiments suggest that results from ordinary density currents are applicable to turbidity currents (Simpson, 1982). In the present study, several models based upon well-known turbulence closures are applied in order to obtain a realistic description of turbidity currents.

MODELS

The equations for U and C given above contain two additional unknowns, the turbulent shear stress τ and the turbulent sediment flux \overline{cw} . The shear stress may be expressed as $\tau = -\rho \overline{uw} + 2(\rho_s - \rho_f)(w_T \cos \beta)^2 C + \rho_s w_T \cos \beta C U$, and turbulence closures are needed for the normal-the-slope fluxes of turbulent momentum \overline{uw} and sediment concentration \overline{cw} .

Boussinesq viscosity model

In Boussinesq viscosity models, the turbulent fluxes are expressed in terms of the mean flow gradients and some specified diffusivity. The results to be reported here are obtained with the use of the well known (k - ϵ) model. Dynamic equations are solved for the turbulent kinetic energy k and the rate of dissipation ϵ of turbulent kinetic energy:

$$\frac{\partial k}{\partial t} = \frac{\partial}{\partial z} \left(\frac{\nu_T}{\sigma_k} \frac{\partial k}{\partial z} \right) + P + G - \epsilon, \quad (3)$$

$$\frac{\partial \epsilon}{\partial t} = \frac{\partial}{\partial z} \left(\frac{\nu_T}{\sigma_\epsilon} \frac{\partial \epsilon}{\partial z} \right) + \frac{\epsilon}{k} (C_{\epsilon 1} P + C_{\epsilon 3} G - C_{\epsilon 2} \epsilon). \quad (4)$$

The fluxes are expressed in terms of k , ϵ and the mean flow gradients as

$$-\overline{uw} = \nu_T \frac{\partial U}{\partial z}, \quad -\overline{cw} = \frac{\nu_T}{\sigma_c} \frac{\partial C}{\partial z}. \quad (5)$$

The diffusivity ν_T (often termed the eddy viscosity) is expressed as $\nu_T = C_\mu k^2/\epsilon$. The coefficients of the model are $(C_\mu, C_{\epsilon 1}, C_{\epsilon 2}, C_{\epsilon 3}, \sigma_c, \sigma_k, \sigma_\epsilon) = (0.09, 1.44, 1.92, 0, 1.0, 1.0, 1.22)$. Further details of this model is given in (Eidsvik and Brørs, 1989) and (Brørs, 1991).

Reynolds stress model

In Reynolds stress models, dynamic equations are solved for \overline{uw} and \overline{cw} , and there is no need for an eddy viscosity. However, several additional unknowns emerge in the Reynolds averaging process. It is the Reynolds normal stresses $\overline{u^2}$, $\overline{v^2}$, $\overline{w^2}$, the concentration flux \overline{cw} and the variance of the concentration fluctuations, $\overline{c^2}$. With the ϵ equation, this adds up to an eight equation model:

$$\begin{aligned} \frac{\partial \overline{u^2}}{\partial t} &= \frac{\partial}{\partial z} \left(C_s \overline{w^2} \frac{k}{\epsilon} \frac{\partial \overline{u^2}}{\partial z} \right) - \frac{\epsilon}{k} \left(C_1 (\overline{u^2} - \frac{2}{3} k) - C'_1 f \overline{w^2} \right) \\ &\quad - \left(2 - \frac{4}{3} C_2 + \frac{2}{3} C_2 C'_2 f \right) \overline{uw} \frac{\partial U}{\partial z} + \left(2 - \frac{4}{3} C_3 + \frac{2}{3} C_3 C'_3 f \right) \overline{cw} g' \sin \beta \\ &\quad - \left(\frac{2}{3} C_3 - \frac{4}{3} C_3 C'_3 f \right) \overline{cw} g' \cos \beta - \frac{2}{3} \epsilon, \end{aligned} \quad (6)$$

$$\begin{aligned} \frac{\partial \overline{v^2}}{\partial t} &= \frac{\partial}{\partial z} \left(C_s \overline{w^2} \frac{k}{\epsilon} \frac{\partial \overline{v^2}}{\partial z} \right) - \frac{\epsilon}{k} \left(C_1 (\overline{v^2} - \frac{2}{3} k) - C'_1 f \overline{w^2} \right) \\ &\quad - \left(\frac{2}{3} C_2 + \frac{2}{3} C_2 C'_2 f \right) \overline{uw} \frac{\partial U}{\partial z} + \left(\frac{2}{3} C_3 + \frac{2}{3} C_3 C'_3 f \right) \overline{cw} g' \sin \beta \\ &\quad - \left(\frac{2}{3} C_3 - \frac{4}{3} C_3 C'_3 f \right) \overline{cw} g' \cos \beta - \frac{2}{3} \epsilon, \end{aligned} \quad (7)$$

$$\begin{aligned} \frac{\partial \overline{w^2}}{\partial t} &= \frac{\partial}{\partial z} \left(C_s \overline{w^2} \frac{k}{\varepsilon} \frac{\partial \overline{w^2}}{\partial z} \right) - \frac{\varepsilon}{k} \left(C_1 (\overline{w^2} - \frac{2}{3} k) + 2 C_1' f \overline{w^2} \right) \\ &\quad - \left(\frac{2}{3} C_2 - \frac{4}{3} C_2 C_2' f \right) \overline{w w} \frac{\partial U}{\partial z} + \left(\frac{2}{3} C_3 - \frac{4}{3} C_3 C_3' f \right) \overline{c u} g' \sin \beta \\ &\quad - \left(2 - \frac{4}{3} C_3 + \frac{8}{3} C_3 C_3' f \right) \overline{c w} g' \cos \beta - \frac{2}{3} \varepsilon, \end{aligned} \tag{8}$$

$$\begin{aligned} \frac{\partial \overline{w w}}{\partial t} &= \frac{\partial}{\partial z} \left(C_s \overline{w^2} \frac{k}{\varepsilon} \frac{\partial \overline{w w}}{\partial z} \right) - \frac{\varepsilon}{k} \left(C_1 + \frac{3}{2} C_1' f \right) \overline{w w} \\ &\quad - \left(1 - C_2 + \frac{3}{2} C_2 C_2' f \right) \overline{w^2} \frac{\partial U}{\partial z} + \left(1 - C_3 + \frac{3}{2} C_3 C_3' f \right) \overline{c w} g' \sin \beta \\ &\quad - \left(1 - C_3 + \frac{3}{2} C_3 C_3' f \right) \overline{c u} g' \cos \beta, \end{aligned} \tag{9}$$

The closed equations for the scalar fluxes and half the variance of the scalar fluctuations are:

$$\begin{aligned} \frac{\partial \overline{c u}}{\partial t} &= \frac{\partial}{\partial z} \left(C_{cs} \overline{w^2} \frac{k}{\varepsilon} \frac{\partial \overline{c u}}{\partial z} \right) - \overline{w w} \frac{\partial C}{\partial z} - \frac{\varepsilon}{k} C_{c1} \overline{c u} - (1 - C_{c2}) \overline{c w} \frac{\partial U}{\partial z} \\ &\quad + (1 - C_{c3}) \overline{c^2} g' \sin \beta, \end{aligned} \tag{10}$$

$$\begin{aligned} \frac{\partial \overline{c w}}{\partial t} &= \frac{\partial}{\partial z} \left(C_{cs} \overline{w^2} \frac{k}{\varepsilon} \frac{\partial \overline{c w}}{\partial z} \right) - \overline{w^2} \frac{\partial C}{\partial z} - \frac{\varepsilon}{k} (C_{c1} + C_{c1}' f) \overline{c w} \\ &\quad - (1 - C_{c3} + C_{c3} C_{c3}' f) \overline{c^2} g' \cos \beta, \end{aligned} \tag{11}$$

$$\frac{\partial \frac{1}{2} \overline{c^2}}{\partial t} = \frac{\partial}{\partial z} \left(C_c \overline{w^2} \frac{k}{\varepsilon} \frac{\partial \frac{1}{2} \overline{c^2}}{\partial z} \right) - \overline{c w} \frac{\partial C}{\partial z} - \varepsilon_c. \tag{12}$$

The model equation for turbulence energy dissipation is

$$\frac{\partial \varepsilon}{\partial t} = \frac{\partial}{\partial z} \left(C_\varepsilon \overline{w^2} \frac{k}{\varepsilon} \frac{\partial \varepsilon}{\partial z} \right) + \frac{\varepsilon}{k} (C_{\varepsilon 1} P - C_{\varepsilon 2} \varepsilon + C_{\varepsilon 3} \max(0, G)). \tag{13}$$

The dissipation of scalar variance is approximated from an assumed constant ratio R between the scalar and dynamic turbulent time scales:

$$\varepsilon_c = \frac{1}{2R} \frac{\varepsilon}{k} \overline{c^2}. \tag{14}$$

In the equations, P and G denote the generation rate of turbulent kinetic energy by the mean velocity gradient and by gravitational effects:

$$P = -\overline{w w} \frac{\partial U}{\partial z}, \tag{15}$$

$$G = \overline{cu} g' \sin \beta - \overline{cw} g' \cos \beta. \quad (16)$$

The function f is a damping function for the wall echo effect on the pressure strain correlations. It is normalized to a value of one near the wall and is expressed by the turbulent length scale ℓ :

$$f \propto \left(\frac{\ell}{z}\right), \quad \ell \equiv \frac{k^{\frac{3}{2}}}{\varepsilon}. \quad (17)$$

The present model is equivalent to the one presented by Gibson and Launder (1977) and the same set of coefficients is used. Further details are given in Brørs (1991) and Brørs and Eidsvik (1992). The model takes into account the proximity or "echo" effect of the bottom on the turbulent stresses. All coefficients with primes in equations (6) to (13) indicate terms with this purpose.

RESULTS

The two-equation (k - ε) model predicts phase plane behaviour in accordance with results from theoretical work reported in the literature, and with limits for auto-suspension within the range of conventional estimates (Eidsvik and Brørs, 1989). However, by its design, this model and simpler gradient diffusion models are unable to produce turbulent diffusion of sediments through the level of the velocity maximum. This feature is considered to be important for the development of turbidity currents, and should be reproduced by a proper model. Modifications of the (k - ε) model with algebraic stress models and algebraic length-scale expressions are made but do not solve this problem. Use of second-moment Reynolds stress turbulence closure (Brørs, 1991, Brørs and Eidsvik, 1992) proves to overcome the problem of vanishing turbulent diffusivity in the velocity maximum, and plausible results for vertical distribution of flow parameters in turbidity currents are obtained. Predictions with the full, eight-equation Reynolds stress model mentioned here compare favourably with available data for this type of flow.

Figure 2 (a) and (b) shows predicted normal-to-the-slope profiles for a turbidity current on a $\beta = 0.05$ radians slope. The flow has been allowed to develop for $t = 320$ seconds, from a 0.3 m high stationary cloud. The sediment grain diameter is 50 μm and the settling velocity is 0.15 cm/s. The initial concentration is $C = 0.3$. At the time shown, the flow has reached a height of about 7 m. The (k - ε) and Reynolds stress models are seen to produce nominally nearly identical velocities, although the former predicts a very pointed velocity maximum. The Reynolds stress model predicts a fuller C profile.

The turbulent kinetic energy k and eddy viscosity ν_T are shown in Figure 2 (c) and (d). For the Reynolds stress model, an eddy viscosity is back-calculated from the prediction using the expression $\nu_T = C_\mu \overline{w^2} k / \varepsilon$, with C_μ being a constant equal to 0.263 and $\overline{w^2}$ the variance of the velocity fluctuations normal to the slope. The dashed line shows the ν_T profile for the (k - ε) model. The eddy viscosity is seen to be zero at the level ($z \sim 0.2$ m) of the mean velocity maximum. Here, the turbulence energy production $P = \nu_T (\partial U / \partial z)^2$ in (3) is zero. The velocity

minimum inhibits the transport of sediments to the outer part of the flow, and a strong density gradient is created at this level. The steep density gradient causes a large negative value for the bouyancy production term $G = g'(\nu_T/\sigma_c)(\partial C/\partial z)$. This reduces k further, it eventually approaches zero, and so does ν_T .

In zero-equation models it is usual to omit the problem by using a so-called "linear bridge", that is by exchanging the portion around the minimum of the ν_T profile with a straight line connecting the maxima on either side. An approach like this has been applied on the present (k - ε) model, both to ν_T and to k . The dashed-dotted lines in Figure 2 show predicted profiles when the dip in the k profile is replaced with a value 0.15 times the near-bottom k maximum value. Although the k bridge is seen to give U and C profile shapes similar to those produced by the full Reynolds stress model, it causes a large (about 50% for the velocity) nominal increase in the values. This could possibly be corrected by changing the model coefficients, although this has not been attempted.

Figure 3 shows a prediction of one of the laboratory saline gravity currents of Ellison and Turner (1959). The profiles are normalized, and $z_{1/2}$ is the level in the outer layer where the velocity is reduced to one half the profile maximum U_m . The Reynolds stress model is seen to be superior to the (k - ε) model in representing this experiment.

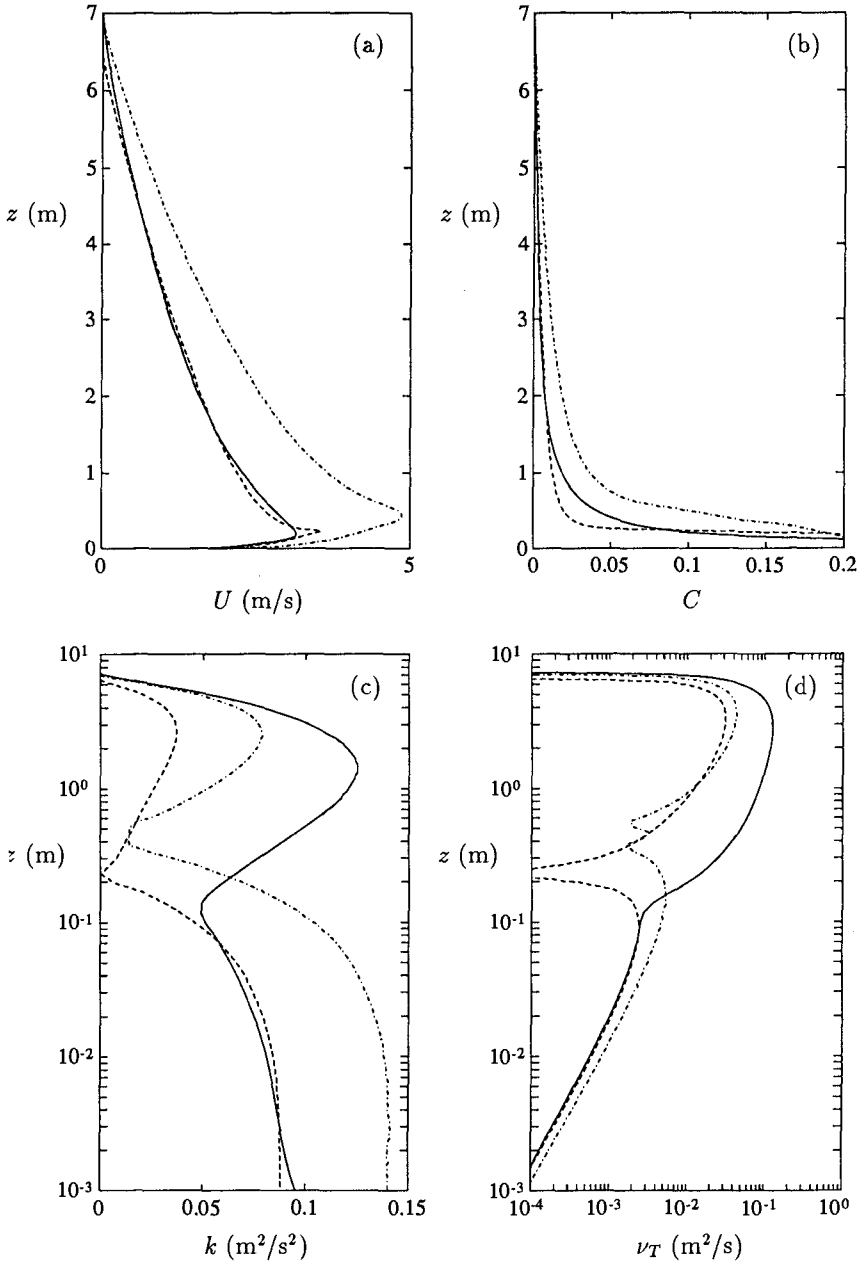


Figure 2: Predicted profiles for self-accelerating turbidity current. Full line; Reynolds stress model, dashed line; $(k-\epsilon)$ model, dashed-dotted line; $(k-\epsilon)$ model with bridge across the k profile dip.

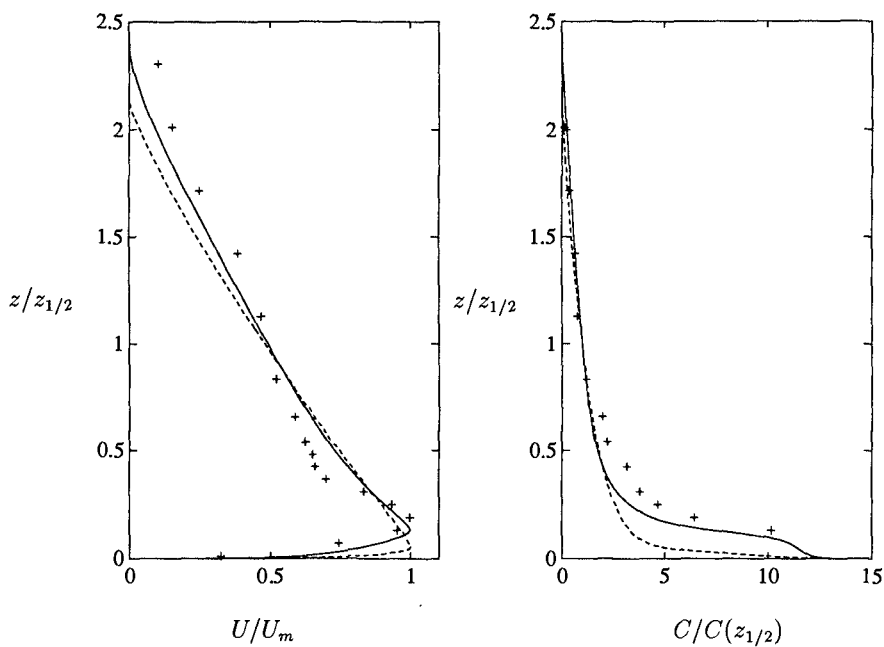


Figure 3: Predicted mean flow profiles for saline gravity current. Symbols represent laboratory experiments by Ellison and Turner (1959). Line types as in Figure 2. The slope is $\beta = 0.24$ radians.

REFERENCES

- Brørs, B. (1991). *Turbidity current modelling*. Dr.ing. thesis, The Norwegian Institute of Technology, Trondheim, Norway. 164 pp.
- Brørs, B. and K. J. Eidsvik (1992). Dynamic Reynolds stress modelling of turbidity currents. *J. Geophys. Res.*, *97*, (C6), 9645-9652.
- Eidsvik, K.J. and B. Brørs (1989). Self-accelerated turbidity current prediction based upon $(k-\varepsilon)$ turbulence. *Cont. Shelf Res.*, *9*, 617-627.
- Ellison, T. H and J. S. Turner (1959). Turbulent entrainment in stratified flows. *J. Fluid Mech.*, *6*, 432-448.
- Gibson, M.M. and B. E. Launder (1977). Ground effects on pressure fluctuations in the atmospheric boundary layer. *J. Fluid Mech.*, *86*, 491-511.
- Seymour, R. J. (1986). Nearshore auto-suspending turbidity flows. *Ocean Engineering*, *13*, 435-447.